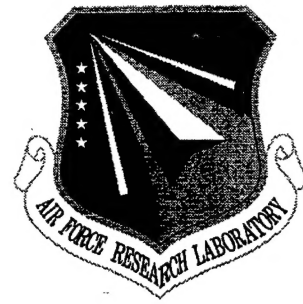


RL-TR-97-208
Final Technical Report
February 1998



MOTIONLESS DYNAMIC SYSTEM FOR 3-D OPTICAL MEMORY BASED ON PLZT ELECTRO- OPTIC LENSES

Syracuse University

Qi Wang Song

APPROVED FOR PUBLIC RELEASE; DISTRIBUTION UNLIMITED.

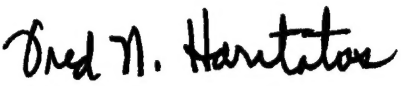
19980324 021


DTIC QUALITY INSPECTED 4

**AIR FORCE RESEARCH LABORATORY
INFORMATION DIRECTORATE
ROME RESEARCH SITE
ROME, NEW YORK**

This report has been reviewed by the Air Force Research Laboratory, Information Directorate, Public Affairs Office (IFOIPA) and is releasable to the National Technical Information Service (NTIS). At NTIS it will be releasable to the general public, including foreign nations.

RL-TR-97-208 has been reviewed and is approved for publication.

APPROVED: 
FRED N. HARITATOS
Project Engineer

FOR THE DIRECTOR: 
JOSEPH CAMERA, Technical Director
Intelligence & Reconnaissance Directorate

If your address has changed or if you wish to be removed from the Air Force Research Laboratory mailing list, or if the addressee is no longer employed by your organization, please notify AFRL/IFED, 32 Hangar Road, Rome, NY 13441-4114. This will assist us in maintaining a current mailing list.

Do not return copies of this report unless contractual obligations or notices on a specific document require that it be returned.

ALTHOUGH THIS REPORT IS BEING PUBLISHED BY AFRL, THE RESEARCH WAS ACCOMPLISHED BY THE FORMER ROME LABORATORY AND, AS SUCH, APPROVAL SIGNATURES/TITLES REFLECT APPROPRIATE AUTHORITY FOR PUBLICATION AT THAT TIME.

REPORT DOCUMENTATION PAGE			Form Approved OMB No. 0704-0188	
<small>Public reporting burden for this collection of information is estimated to average 1 hour per response, including the time for reviewing instructions, searching existing data sources, gathering and maintaining the data needed, and completing and reviewing the collection of information. Send comments regarding this burden estimate or any other aspect of this collection of information, including suggestions for reducing this burden, to Washington Headquarters Services, Directorate for Information Operations and Reports, 1215 Jefferson Davis Highway, Suite 1204, Arlington, VA 22202-4302, and to the Office of Management and Budget, Paperwork Reduction Project (0704-0188), Washington, DC 20503.</small>				
1. AGENCY USE ONLY (Leave blank)	2. REPORT DATE February 1998	3. REPORT TYPE AND DATES COVERED Final Sep 94 - Jun 97		
4. TITLE AND SUBTITLE MOTIONLESS DYNAMIC SYSTEM FOR 3-D OPTICAL MEMORY BASED ON PLZT ELECTRO-OPTIC LENSES		5. FUNDING NUMBERS C - F30602-94-C-0260 PE - 63726F PR - 3192 TA - 00 WU - 08		
6. AUTHOR(S) Qi Wang Song				
7. PERFORMING ORGANIZATION NAME(S) AND ADDRESS(ES) Syracuse University 121 Link Hall Syracuse NY 13244-1200		8. PERFORMING ORGANIZATION REPORT NUMBER N/A		
9. SPONSORING/MONITORING AGENCY NAME(S) AND ADDRESS(ES) AFRL/IFED 32 Hangar Road Rome NY 13441-4114		10. SPONSORING/MONITORING AGENCY REPORT NUMBER RL-TR-97-208		
11. SUPPLEMENTARY NOTES AFRL Project Engineer: Fred N. Haritatos/IFED/(315) 330-4582				
12a. DISTRIBUTION AVAILABILITY STATEMENT Approved for public release; distribution unlimited.		12b. DISTRIBUTION CODE		
13. ABSTRACT (Maximum 200 words) The objective of this effort is to design, fabricate, and test a device that uses the electro-optic effort for laser beam focusing and beam steering. The technology is applicable to standard and next-generation optical disk subsystems and 3-D volumetric optical memories. The report presents experimental results of a two-dimensional electro-optic dynamic diverging lens. The device is based on a lanthanum-modified lead zirconate titanate (PLZT) ceramic wafer. The continual change of focal length is achieved by an applied control voltage. The design of the device takes a simple form and is almost free of diffraction loss.				
14. SUBJECT TERMS Computer Storage, Optical Memory, System Architecture		15. NUMBER OF PAGES 48		
		16. PRICE CODE		
17. SECURITY CLASSIFICATION OF REPORT UNCLASSIFIED	18. SECURITY CLASSIFICATION OF THIS PAGE UNCLASSIFIED	19. SECURITY CLASSIFICATION OF ABSTRACT UNCLASSIFIED	20. LIMITATION OF ABSTRACT UL	

Table of Content

1. Introduction	2
2. The concept of a 3-D optical memory	5
3. Drawbacks of the sheet-of-light concept and the pulse collision with counter-propagating waves	7
4. Scanning line-of-light concept and the PLZT dynamic lens	10
5. Fabrication and analysis of the PLZT electro-optic lens	13
6. Scaleless dynamic imaging system: optical memory recording and retrieval	34
7. Discussions and conclusions	37
8. References	38

1. Introduction

Information storage and retrieval technique is the backbone of any information system. Huge data flow has become common for today's database and multimedia applications and has been made possible because of the development and improvement of memory techniques. There has been an ever-increasing need to rapidly store and retrieve large amount of information of a variety forms including both digital and analog signals. Conventional memory technique has been improved dramatically over the past years. Even for a personal computer the installed hard disk's storage capacity can be several to tens of gigabytes. Optical CD ROM also becomes an important part of today's computers due to its high capacity, low cost and removability. However the serial reading and transfer mode has become a bottle-neck for future high quality, high performance digital applications, such as multimedia and video on demand, and military and industrial object classification and recognition applications. Optical three-dimensional (3-D) memory^{1,2} has been regarded as a potential candidate for overcoming this limitation. 3-D memories offer higher capacity and use parallel means to record and retrieve data and thus are superior to the serial methods.

In 3-D memories, data are stored according to a position described by a 3-D coordinate system, which can be defined as the physical spatial locations in the recording media. Higher dimensional memories may also include other state parameters, such as the wavelength or the polarization status of the light, with which the data is stored and must be retrieved with the same settings. Optics provides an easy way for parallel access and process of the data. Most 3-D optical memories store and retrieve data in image-by-image formats. This greatly increases the capacity and the data transfer rate. 3-D recording and retrieving need dynamic imaging, which controls the light inside the data recording media and enables the information to be stored in different physical locations and to be retrieved accordingly. Conventional lenses have very good specifications for accurate imaging but are bulky and unchangeable if no mechanical adjustment is performed. Conventional zoom lens performs the above task well but its operation is very slow. Currently, dynamic

imaging for 3-D memories is done by mechanical movement of the storage media or the adjustments/replacement of other elements. Therefore the fast accessibility of 3-D optical memories is kept from being fully implemented.

Electro-optic effect has the advantage of fast operation due to the fact that optical properties of the operational materials are changed by means of electrical voltage applied onto the material. There is no need for mechanical adjustment during the operation. Solid ferroelectric electro-optic materials have fast response times and good physical stability. Lanthanum-modified lead zirconate titanate (PLZT)³ is a ferroelectric ceramic material that, with a proper composition, can have a strong quadratic electro-optic effect. The material has been investigated for applications due to its attractive properties. In comparison with electro-optical crystals, PLZT has a larger electro-optical coefficient and is less expensive, especially when a large size is required. When compared with liquid crystals, PLZT offers better physical stability and sub-microsecond time response. The promising electro-optic properties of PLZT opens up the possibilities to develop integrated electro-optical devices for optical beam modulation, steering, and adaptive imaging. Electro-optic lenses,⁴⁻⁶ both variable focal length lenses and dual focal point lenses, made with PLZT show a large dynamic range for the focal plane variation. With the application of voltages of 200 V to 300 V, the focal lengths of the electro-optic lenses can be tuned from tens of centimeters to infinity. This provides a potential application area for electro-optic dynamic lenses. Electro-optic lens can image an input image onto different location inside a 3-D recording media by controlling the applied voltage on the device. But in these efforts, interdigital electrodes were deposited on the PLZT wafer surfaces to apply the required electrical field to the wafer. The intrinsic grating structure of the interdigital electrodes generate an induced overall phase distribution that is not smooth. This stepwise index distribution is acceptable in grating type applications. However, in the applications such as dynamic lenses or prisms, using the stepwise index distribution to approximate the required index distribution induces diffraction, which reduces the light efficiency of the device and produces unwanted noise. In 3-D memory, the unwanted high order diffraction of the grating structure of a zoom lens's electrodes may interfere with the imaging beam and deteriorate the image quality.

We have fabricated a PLZT ceramic based electro-optic dynamic diverging lens.^{7,8} It uses the intrinsic quadratic property of the PLZT's electro-optic effect. Therefore, only a linear electrical field distribution was required to induce the required quadratic modulation in the device. The design offers a single and compact structure that produces a smooth phase modulation distribution. The diverging power of the lens is controlled by the applied voltage. There is little diffraction loss due to the simple electrode arrangement instead of grating-like electrodes, which diffracts considerable light into high diffraction orders, thus it prevents the interference among the diffraction orders. It is a continuous refractive device rather than a phased array device, thus its far field diffraction pattern is like that of a conventional divergent lens. The quadratic nature of its electro-optic effect also enables the device to approach an ideal aberration-free lens. We describe a PLZT ceramic based electro-optic lens, the principle, the device design, fabrication, experimental test, its application to dynamic imaging for optical memory, and computer digital evaluation of the device aberration and correction method. This investigation proves that with minimal modifications the device can be well approximated by an ideal lens. The two fabricated dynamic lenses consist of three thin metal electrodes on the top surface layout and have working areas of $2\text{ mm} \times 2\text{ mm}$ and $3\text{ mm} \times 3\text{ mm}$, respectively. It demonstrates a continuous variable focal length from infinity with no applied voltage to negative 0.77 m with a voltage of 400 V.

In this report, we will briefly review the 3-D optical memory concept, analysis some of the system approaches and then provide our solutions based on the PLZT lenses. The design, fabrication and test of the lens will be detailed in this report.

2. The concept of a 3-D optical memory

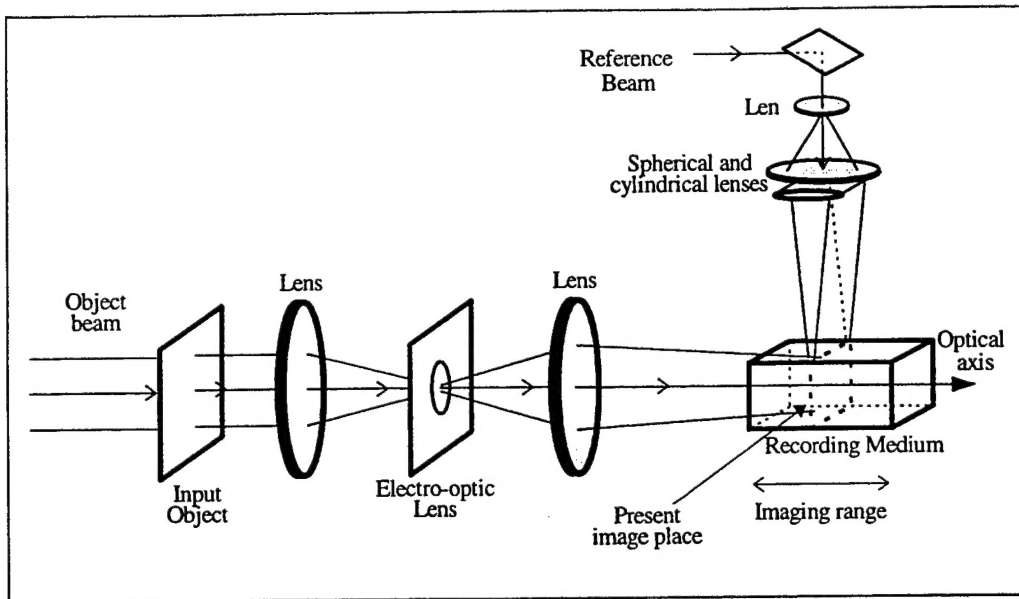


Figure 1. A 3-D optical memory information storage and retrieval.

The above figure shows a typical system for two-photon absorption 3-D optical memory. The object beam is used as the information carrier when it transmits through the input object which can be a display on a transmission spatial light modulator (SLM). The object is imaged onto the recording medium by a combination of lenses including a variable focus-length lens on the Fourier plane. The reference beam is the other arm of the system for the two-photon absorption photochromic recording of information. Reference beam produces a sheet of light covering the image plane of the SLM. When the variable focus-length lens adjusts its focal length, the image plane of SLM shifts along the optical axis in the recording medium. The light sheet traces the image plane. Thus information can be recorded in the medium page by page. The page information storage capacity in the media is limited by the thickness of the sheet-of-light. At the present state, the reported scheme does not have a dynamic imaging system and a scanning sheet-of-light. The mechanism is demonstrated by moving the recording medium.

Three dimensional memories can be implemented by other means, such as wavelength and angular multiplexing. The storage spaces for wavelength and angular multiplexing are overlapped in the recording medium, thus suffering low recording and diffraction efficiencies. As it is not related to this report, we will not go into the details.

3. Drawbacks of the sheet-of-light concept and the pulse collision with counter-propagating waves

The sheet-of-light concept was proposed, as mentioned in previous section, for the page-by-page optical recording in a cubic memory media, which was to be used to envelope the image plane of the to-be-recorded page of information. By nature it is produced from a laser, thus it is governed by the Gaussian beam property.

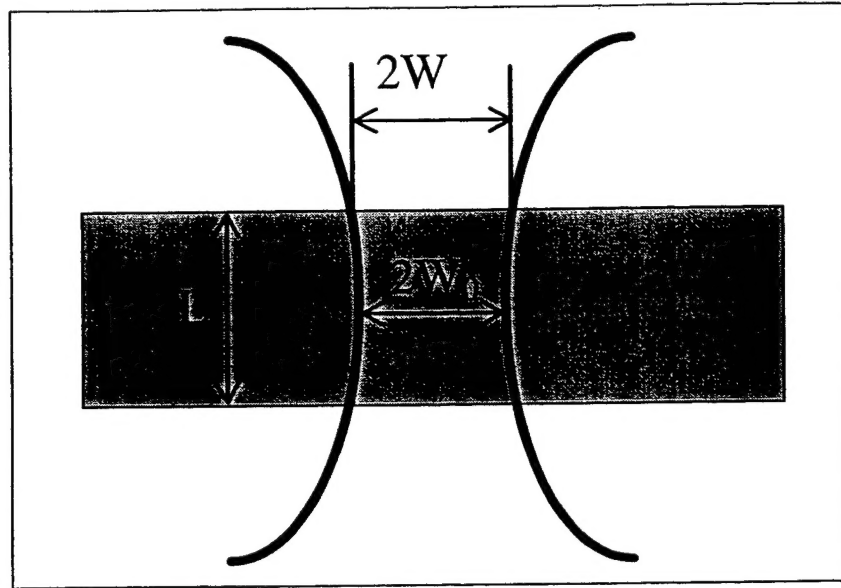


Figure 2. Propagation of Gaussian beam in a recording media.

As shown in Figure 2, if we would like a sheet-of-light with a thickness, $2W_0$, at its waist position, the sheet thickness, $2W$, at the front and back surface of the recording media will satisfy

$$W^2 = W_0^2 + \frac{L^2}{k_0^2 n_0^2 W_0^2} \quad (3-1)$$

where L is the thickness of the recording media, k_0 is the wave vector of the illuminating light and n_0 is the refractive index of the media. W determines the thickness of the

information recording layer and hence the recording density. So we are to find an as-small-as-possible W , which is a function of W_0 , provided that other parameters in Eq. (3-1) are fixed. The W we are looking for satisfies

$$\frac{\partial(W^2)}{\partial(W_0^2)} = 1 - \frac{L^2}{k_0^2 n_0^2 W_0^4} = 0 \quad (3-2)$$

That is

$$W_0^4 = \frac{L^2}{k_0^2 n_0^2} \quad (3-3)$$

Considering a practical situation, we choose $L = 1.0 \text{ cm}$, $k_0 = \frac{2\pi}{\lambda} = \frac{2\pi}{0.633} \mu\text{m}^{-1}$ and $n_0 = 1.5$. Thus we have

$$2W_0 \cong 52 \mu\text{m} \quad (3-4)$$

$$2W = 2\sqrt{2}W_0 \cong 73 \mu\text{m} \quad (3-5)$$

So far we all consider the perfect condition and do not include any device or system limitations. This is a restriction caused by the 3-D recording nature, determined by the size of the recording material. Any attempts to better this limitation are beyond the physics principles.

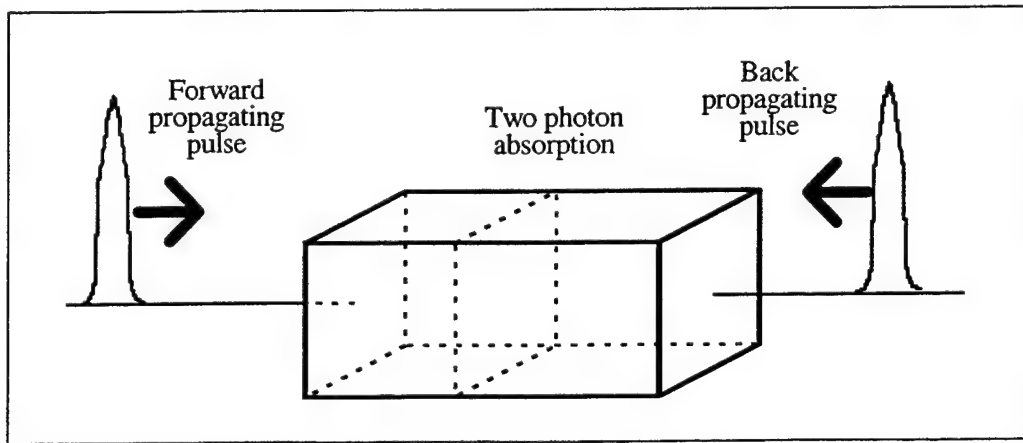


Figure 3. Concept of counter-propagating pulses.

Counter-propagating pulse collision for two-photon absorption optical memory was another approach. Suppose there are two short light pulses traveling in opposite directions. When they meet in the recording medium, two-photon absorption occurs, thus information recording is performed. The delay between these two pulses can be precisely adjusted to have the collision takes place in any position inside the recording medium. To be compatible at least with the sheet-of-light concept, the pulse should have pulse length (width), Δ , not longer than $73 \mu\text{m}$, which is corresponding to a light duration of

$$t = \frac{\Delta}{v} = \frac{73 \mu\text{m} \times 1.5}{3.0 \times 10^{14} \mu\text{m/s}} = 3.7 \times 10^{-13} \text{ s}, \quad (3-6)$$

where v is the speed of light in the medium. This requires sub-picosecond pulses, which requires bulk and state-of-art equipment to generate. To be considered a better approach, the pulse width should be much shorter than this number. Also there exists a problem for the retrieval of the information recorded.

4. Scanning line-of-light concept and the PLZT dynamic lens

The fundamental limitation of sheet-of-light, although the process is massive parallel, limits the information recording density in the media. As an alternative, we proposed the concept of scanning line-of-light. We just use the fine linear portion at the waist position of the “sheet-of-light” (Figure 1). We need not to consider the sheet-of-light thickness at the surface of the recording material any more but the waist size. The waist size can be formed much small as we will see later in this report. The information recording is performed line by line instead of page-by-page. Although sort of parallelism is sacrificed compared with the later, the line-by-line recording still maintains a very high parallelism compared with the current bit-by-bit serial method by today’s computer industry. And because the line-of-light can be very thin (only limited by the real system design), high recording density is surely promised.

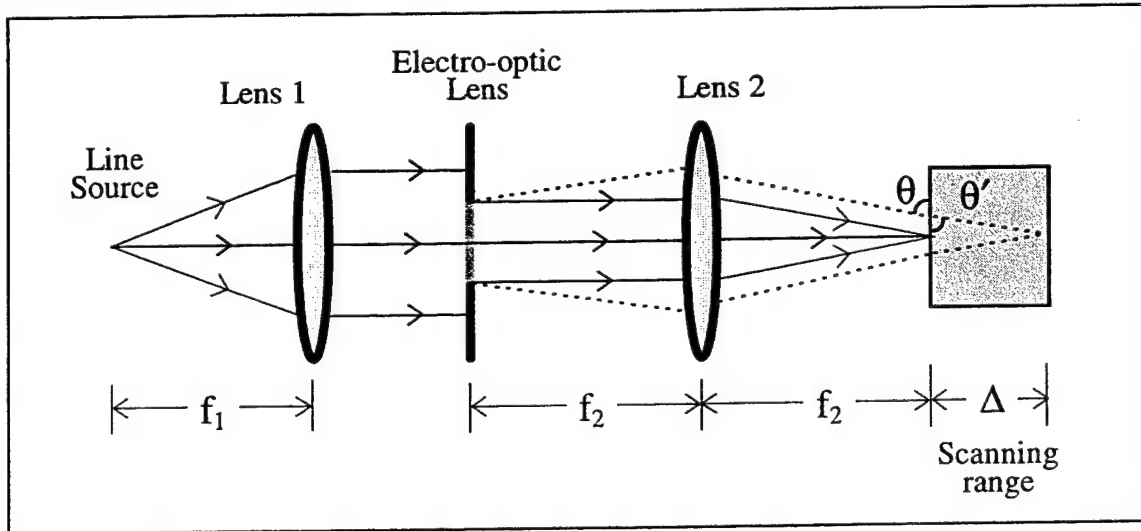


Figure 4. The scanning line of light approach for reference beam.

The setup to generate the scanning line of light is illustrated in Figure 4. A line source is assumed at the left end of the figure, with the line of light perpendicular to the surface of the page. A very fine line of light, in the range of micron or sub-micron, can be easily generated using conventional optical systems, which is not shown in this figure.

Lens 1 is used to collimate the light in the shown dimension. A variable focal-length lens is used to performed the scanning. We have fabricated inexpensive PLZT ceramic-based electro-optic lenses,^{7,8} which can take this role. When there is no voltage applied on PLZT lens, the lens acts just like an aperture. Lens 2 is used to reform the image of the line source onto its back focal plane. The line image width is expressed as

$$l = \frac{2(nf_2)\lambda/n}{W} = \frac{2f_2\lambda}{W} \quad (4-1)$$

where λ is the wavelength of the source in vacuum, n is the refractive index of the medium, and W is the aperture size of PLZT lens.

When a voltage is applied onto the PLZT lens, the output line-of-light will move along the optical axis of the system. Suppose, under certain voltage, the diverging electro-optic lens has a focal length of f_0 , then the scanning range Δ will satisfy

$$\frac{\Delta}{n} = \frac{f_2^2}{f_0} \quad (4-2)$$

Our fabricated PLZT lens has a working window of 2 mm and a focal length of 0.77 meter under a voltage of 400 V. If we need the line scanning range being 1 cm, the focal length of Lens 2 can be chosen as

$$f_2 = \sqrt{\frac{\Delta \cdot f_0}{n}} = \sqrt{\frac{1 \text{ cm} \cdot 77 \text{ cm}}{1.5}} = 7.2 \text{ cm} \quad (4-3)$$

So the line image width is

$$l = \frac{2 \times 72 \times 0.633}{2} \mu\text{m} = 45 \mu\text{m} \quad (4-4)$$

This width remains constant as the voltage varies. Further improvements require wider lens aperture, shorter wavelength or shorter focal length of f_2 hence f_0 . These are all achievable with the current technology. We have had several larger lens but needs a little higher voltage to operate. Stacking two or more such lenses can double the numerical aperture of the PLZT lens and reduce the working voltage. Besides, the measured focal length of the above assumed PLZT lens is 50% longer than the theoretical prediction. This is due to the imperfection of the material or/and the fabrication technique. Thus a technical improvement on fabrication can improve the performance significantly. PLZT

material are still under intensive development, we are confident that in the future new finding or result will strengthen our claim of this light scanning concept. With current techniques we have for our fabrication, a line width of the scanning line-of-light under 10 μm is achievable.

In 3-D optical memory, the line-of-light and a line of information intersects inside the media. The recording only occurs in the intersection, such as in two-photon absorption. The recording density is determined by both the line-of-light width and the information density on an input image. The PLZT lens operates in a very fast manner, several microseconds, thus fast recording is guaranteed.

5. Fabrication and analysis of the PLZT electro-optic lens

PLZT is polycrystalline, which is prepared from PLZT powder by hot press in a temperature more than 1000°C. It can be prepared in any size or shape. Without an external field PLZT exhibits an isotropic optical property, with an intrinsic refractive indices of $n_0 = 2.5$. PLZT ceramic is quite transparent for a large range of wavelength. But due to its high intrinsic refractive index PLZT wafer has an intrinsic transmittance of 67% caused by its surface reflections.⁹ With proper anti-reflection coating on the surface, the transmittance can be increased as high as 98%. PLZT has large quadratic electro-optic coefficients. When PLZT is placed in an electrical field, its index of refraction changes according to the following principle

$$\Delta n_x(x, y) = -\frac{1}{2}n_0^3 R_{11} E^2(x, y), \quad (5-1)$$

$$\Delta n_y(x, y) = -\frac{1}{2}n_0^3 R_{12} E^2(x, y), \quad (5-2)$$

$$\Delta n_z(x, y) = -\frac{1}{2}n_0^3 R_{12} E^2(x, y), \quad (5-3)$$

where Δn_x , Δn_y and Δn_z refer to the refractive index changes when the polarization of the light is parallel to the electrical field direction and the other two perpendicular to the electrical field and each other, R_{ij} indicates the quadratic electro-optic (Kerr) coefficients, and we have taken the electrical field direction as the x-axis.

PLZT's electro-optic coefficient can be different if the lanthanum concentration changes. The material PLZT 9/65/35 has a 65:35 ratio of PbZrO_3 to PbTiO_3 with a lanthanum concentration of 9%. Numerical values of the Kerr coefficients in the literature^{4,5} are $R_{11} = 4.00 \times 10^{-16} \text{ m}^2/\text{V}^2$ and $R_{12} = -2.42 \times 10^{-16} \text{ m}^2/\text{V}^2$.

5.1) Device design and its working principles

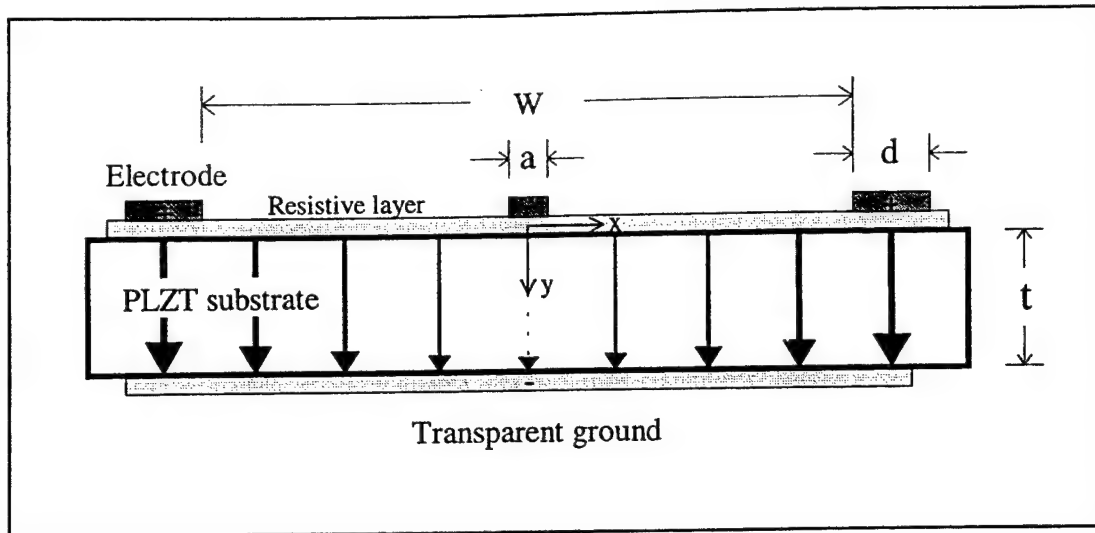


Figure 5. Cross-sectional view of the PLZT-based electro-optic variable cylindrical lens.

Figure 5 shows the cross-sectional view of the designed cylindrical electro-optic dynamic diverging lens. Corresponding design parameters are noted on the figure. The structure on the top surface consists of three parallel metal electrodes and a transparent resistive layer. A transparent conductive film, which serves as ground, is on the back surface of the PLZT substrate. The two outer electrodes on the top surface are connected together to one of the power supply contacts. The central one and the back surface ground terminal are connected to the other contact of the supply. The resistive layer on the top surface, with a properly selected sheet resistance, is used to provide a continuous and linear potential distribution between the central and the outer electrodes. The result is a compact device with only two external electrical contacts. Figure 5 also depicts the resultant electrical field distribution with the stronger field denoted by thicker arrows. For simplicity, the relative weak inter-electrode field is ignored in the illustration. This device takes advantage of the longitudinal electro-optic effect so that the electro-optic interaction length is equal to the thickness of the PLZT substrate. The advantages of using the longitudinal effect, as compared to using the transverse effect, is that it is polarization independent.⁷ Therefore, two such one-dimensional (1-D) cylindrical devices can be stacked in tandem to provide a 2-D dynamic lens. This simple wiring is advantageous in

comparison with many dynamic electro-optical beam focusing/steering devices that require complicated external wiring which are cumbersome and prone to malfunctions. A more precise derivation that involves solving a two-dimensional Laplace equation and the index ellipsoid of the electro-optic effect in the PLZT ceramic will be presented later in this section.

First of all, we define the coordinate system. Principal axes x and z lie in the top surface of the PLZT substrate and are arranged perpendicular and parallel to the electrodes respectively. Axis y points into the PLZT wafer as indicated in the figure. To design the device, we assume a simplified mathematical mode. The induced change in refractive index of the PLZT 9/65/35, for the case where the incident beam is in the direction of the electrical field, is given by⁵

$$\Delta n = -\frac{1}{2} n_0^3 R_{12} E^2, \quad (5-4)$$

where n_0 is the intrinsic refractive index of PLZT, R_{12} is the quadratic PLZT Kerr coefficient and E is the external electric field. For the 633nm He-Ne laser wavelength, n_0 is 2.5 and $R_{12} = -2.42 \times 10^{-16} \text{ m}^2/\text{V}^2$. The uniform resistant layer produces a linear potential distribution between the outer and central electrodes. Because of the one-dimensional nature of the electrodes distribution, the three-dimensional electrical field distribution inside the PLZT substrate can be simplified into a two-dimensional case, that is the x - y distribution. We select the central electrode as the origin and the direction perpendicular to the electrodes on the top PLZT surface the x axis. The induced electrical field inside the PLZT is

$$E(x) = \frac{2V}{Wt} |x|, \quad (5-5)$$

where $|x|$ denotes the absolute value of the x coordinate, W stands for the width of the device, t represents the thickness of the PLZT substrate and V is the applied voltage. This electrical field is parallel to the incident beam. So after passing through the PLZT wafer, the beam experiences a light path modulation that is then resulted

$$\Delta l(x) = -\frac{2n_0^3 R_{12} V^2}{W^2 t} x^2. \quad (5-6)$$

This process is depicted in Figure 6.

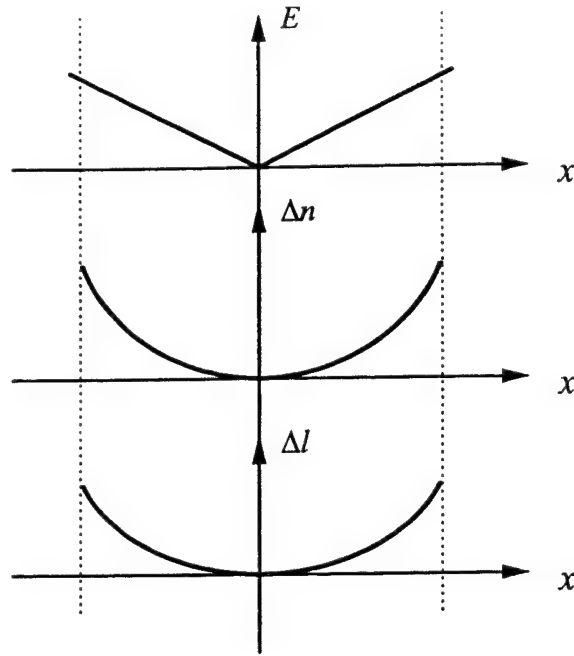


Figure 6. Working principle for transmission light.

This modulation implies a diverging lens, which is controllable by the applied voltage. The equivalent focal length is

$$f = \frac{W^2 t}{4n_0^3 R_{12} V^2}. \quad (5-7)$$

Here R_{12} is negative, and thus f is negative. For a fixed device effective width and required focal length, the applied voltage can be reduced by decreasing the thickness of the PLZT substrate or choosing a material with a larger quadratic coefficient.

5.2) Device fabrication issues

A 0.32-mm-thick PLZT wafer was used as the substrate for device fabrication. Devices were fabricated with amorphous germanium for the resistive layer, aluminum for the electrodes on the top surface and transparent indium tin oxide (ITO) for the ground on the bottom surface. The thickness of the amorphous germanium layer is 30 nm and was

uniformly evaporated over the whole working area of the PLZT ceramic substrate. The resultant sheet resistivity of the germanium is 258 M Ω /square. This layer produces a linear voltage distribution between the electrodes. The electrodes were made by evaporating aluminum over the germanium resistive layer. Image reversal and wet chemical resist strip-off techniques were employed in electrode deposition. The width of the central electrode is 4 μ m and that for the outer electrodes is 100 μ m. Since the opaque central electrode is in the illuminated region, using a narrower one reduces the loss of the blocked energy. Ideally, utilizing a thin and transparent central electrode the loss of the energy will be kept to a minimum. However, ITO, which is the only available material to us, has a surface resistance of approximately 47 Ω /square which is too large for this application. Fortunately, we found in the experiment that the energy loss and the diffraction due to the 4 μ aluminum electrode were negligible. The spacing between the central and the outer electrodes is 1 mm, i.e., the result is a 2-mm-wide cylindrical variable lens. On the back side of the substrate, a 130 nm thick ITO layer was deposited by a sputtering method in order to serve as the ground terminal, to which the central electrode on the front surface of the PLZT was connected. Lenses with width of 3 and 4 mm respectively were also fabricated.

5.3) Experimental test of the device and its application in dynamic imaging

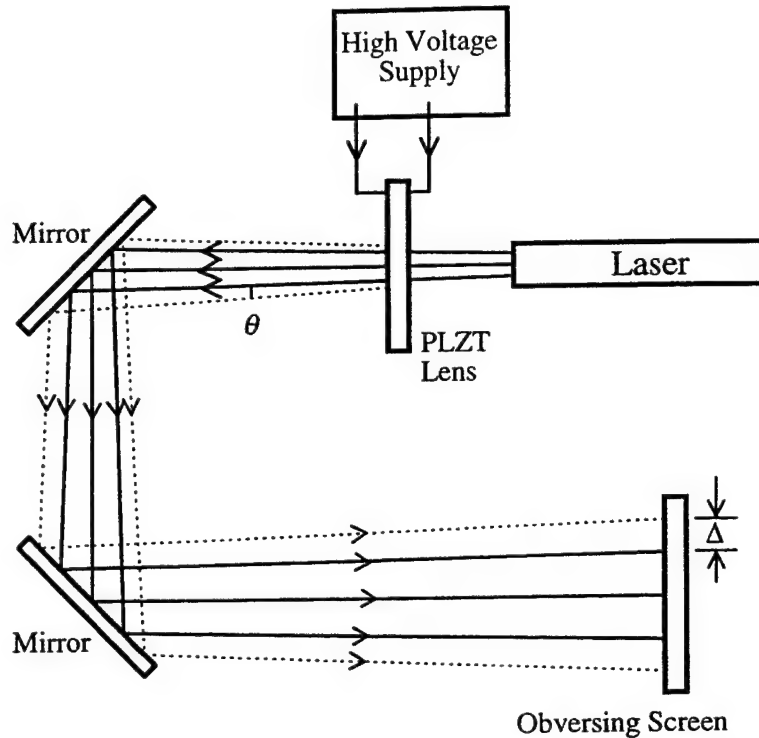


Figure 7. Experimental setup for the beam diverging observation and diverging angle measurement.

To perform the experimental test, an experimental system was set up, as illustrated in Figure 7. A linearly polarized He-Ne laser beam of 633nm was incident normal to the device surface. A high voltage power supply was used to generate a voltage of up to 400V. The transmitted beam was examined at a certain distance behind the device. When voltages of 200V and 400V were applied, half diverging angles of 0.02 and 0.08 degrees respectively, were measured by comparing the far field light spots when the electrical power was on and off. Equivalent local lengths were then determined to be -3.25 and -0.77 meters, respectively. Figure 8 shows the diverging far field patterns. They are almost pure refractive patterns with slight diffraction effects caused by edges of the electrodes.

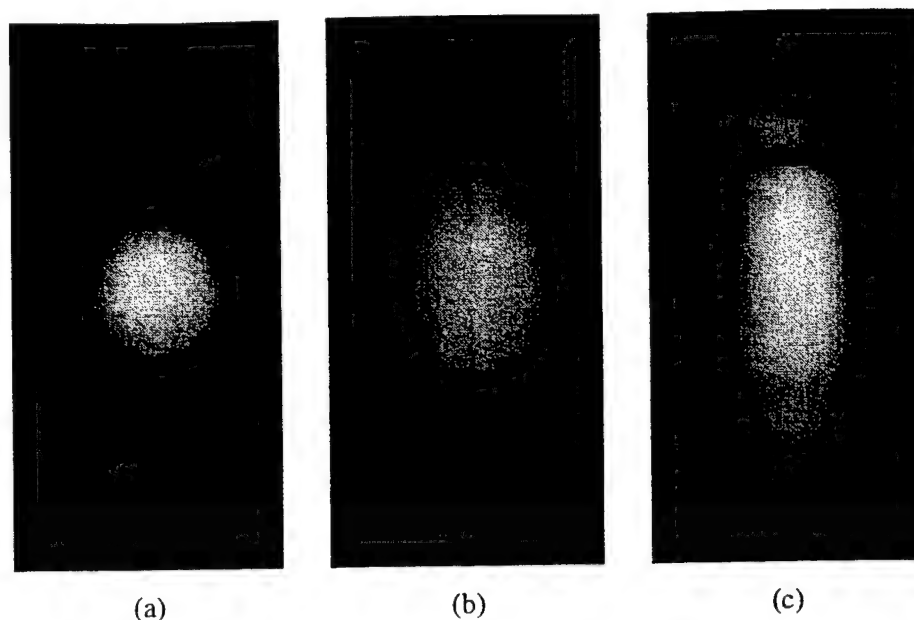


Figure 8. Far-field patterns of a laser beam passing through the device (a) without the external source, (b) with an applied voltage of 200 V, and (c) with an applied voltage of 400 V.

By entering an addition converging spherical lens in front of the dynamic lens, this lens can be used just like that of the Sato lens⁵ but our device still enjoy the advantages listed in the introduction section of this report. A positive convenient lens is easy to be fit onto the electro-optic lens. The modified experimental setup is shown in Figure 9.

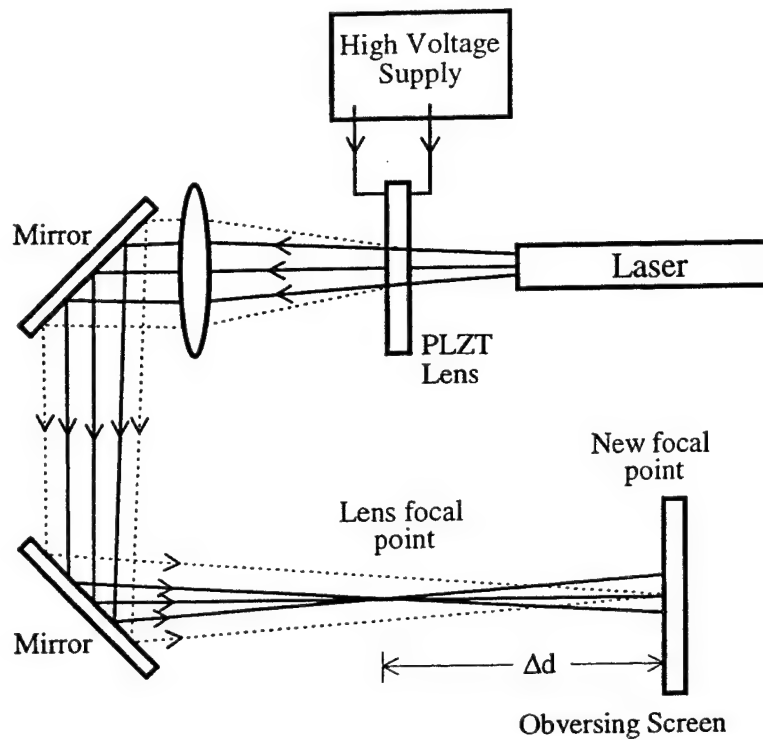


Figure 9. Setup for dynamic focusing test and measurement.

We examined the combined focusing effect in this setup. Figure 10 gives the patterns obtained at a proper plane for the cases where the applied voltages is 0 V, 200 V, and 400 V, respectively.

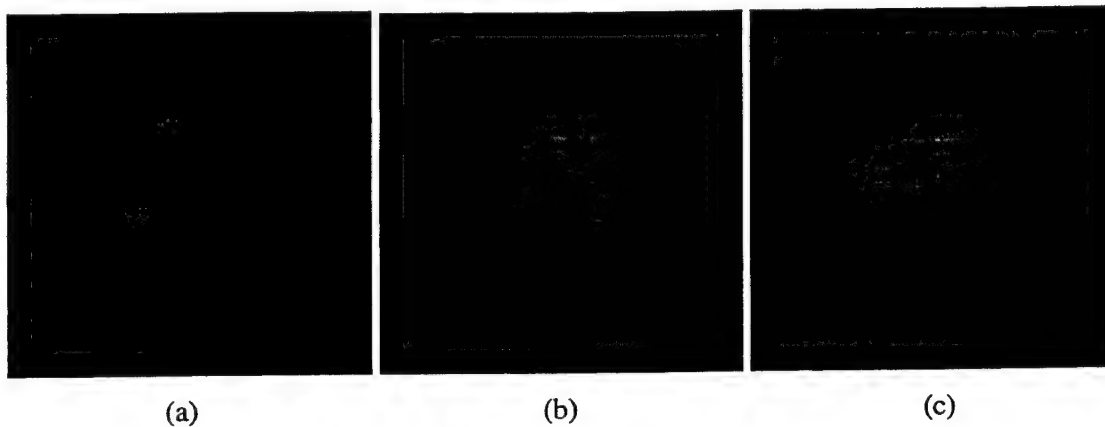


Figure 10. Focusing effect of the device combined with a converging lens (a) without the external source, (b) with an applied voltage of 200 V, and (c) with an applied voltage of 400 V.

It is noted that because of the use of longitudinal electro-optic effect, the dynamic lens is insensitive to the polarization of the incident laser beam. So a two-dimensional modulation can be achieved by placing in tandem two identical one-dimensional lenses that are oriented perpendicularly as shown in Figure 11.

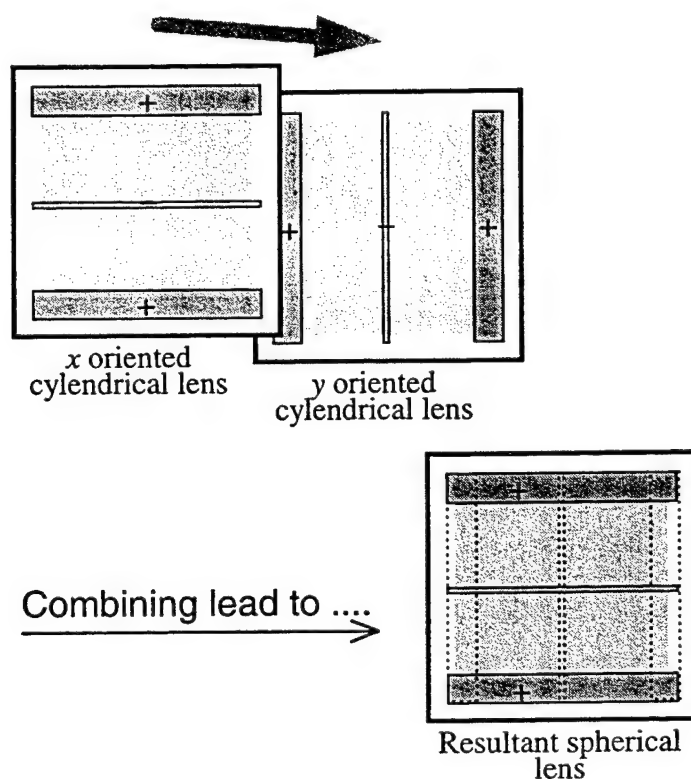


Figure 11. Forming a two-dimensional lens.

This cascaded two-dimensional modulation is not achievable in most previously reported results where transverse electrical modulations were used. In addition, since the diverging powers of the two cylindrical lenses can be controlled either independently or synchronized, the combined device offers the performance flexibility which are very useful in many adaptive asymmetric imaging or focusing applications. Two identical 1-D lenses were used for this purpose.

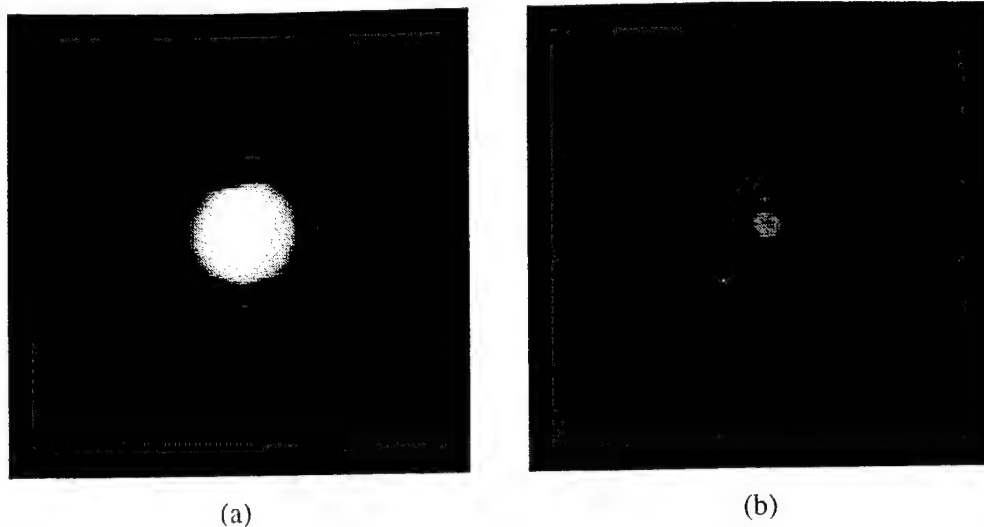


Figure 12. Two-dimensional focusing effect with a $2\text{mm} \times 2\text{mm}$ lens composed by two crossed dynamic cylindrical lenses put back to back (a) without the external source and (b) with an applied voltage of 400 V. The pictures are taken at the focal plane of the device that is illuminated by a Gaussian beam.

Figure 12 shows the focusing effect by this combined electro-optic lens, which has an effective working area of $2\text{mm} \times 2\text{mm}$. These pictures were taken at the focal plane of the combined focal plane of the device and a conventional converging lens. The illumination was a Gaussian beam. The applied voltage is 400 V, and the focal length of the device is -0.77 meters. Values of the quadratic coefficients of PLZT 9/65/35 differ greatly from report to report.¹⁰ In some cases the coefficient is much larger than the one we used. We believe that with a proper composition of materials that produces a larger coefficient R_{12} , and with a thinner substrate, the working voltage can be dramatically decreased.

Experimental observations on its dynamic imaging properties were also conducted. A typical dynamic imaging experimental arrangement consists of an input plane for the display of the to-be-stored images and an imaging lens or lenses combination. A spatial light modulator is a common way used for image input into an optical system. For simplicity in the demonstration, we used a transparency of resolution

chat. The key element of the system is the lens, which can be a single movable/changeable lens or a combination of several lenses.

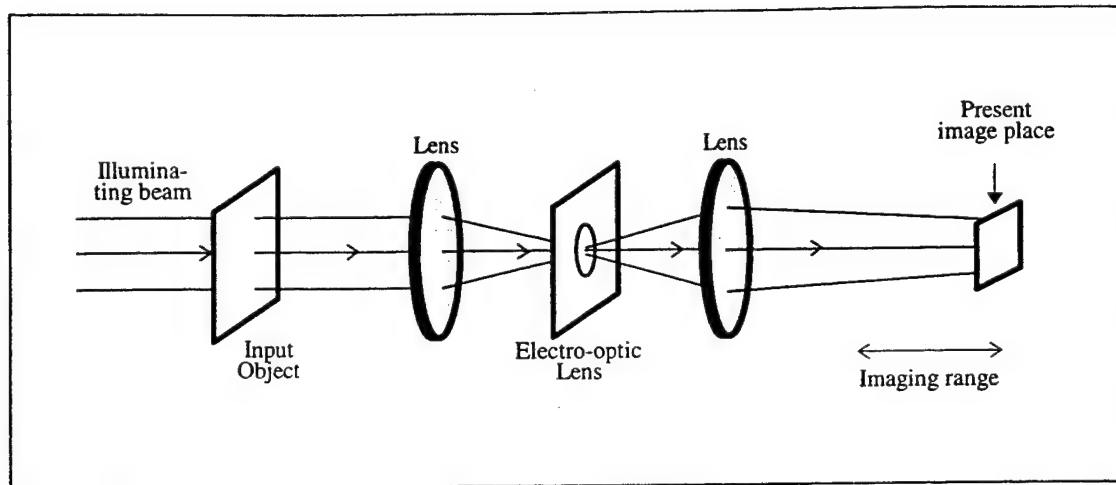
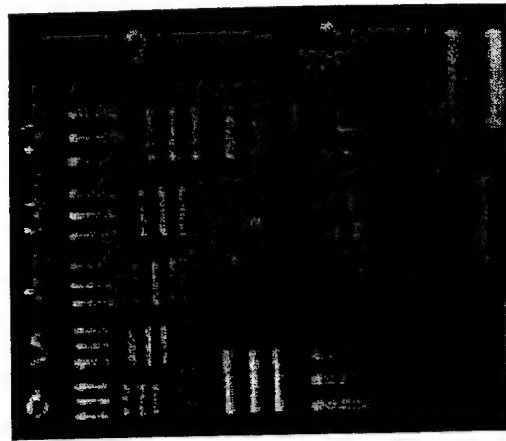
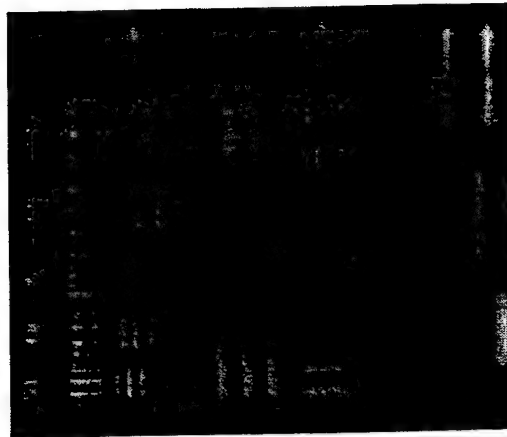


Figure 13. Illustration for dynamic imaging arrangement in the experiment.

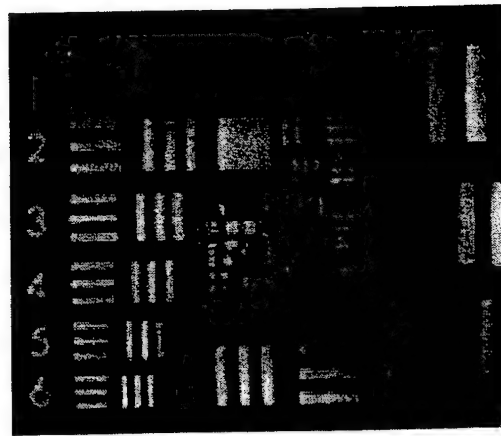
Figure 13 depicts our demonstration system, where the function of two-dimensional variable converging lens is completed by combining two conventional lenses and one two-dimensional PLZT lens. The electro-optic lens is placed at the focal point of the first convenient lens. Dynamic imaging is fulfilled by changing the electro-optic lens. When a certain voltage is applied to the electro-optic lens, its focal length changes according to the voltage value and the electro-optic effect. The resultant focal length of the combined lens is changed, hence the image plane is moved along the optical axis. For a 3-D optical memory, the desired dynamic imaging range is the depth of the recording media. Therefore the requirement for the working voltage range is calculated accordingly.



(a)



(b)



(c)

Figure 14. Two-dimensional dynamic imaging by (a) a 2mm×2mm lens with an applied voltage of 240 V, (b) a 2mm×2mm lens without external source, and (c) a 3mm×3mm lens with an applied voltage of 330 V. Other parameters remains the same.

Figure 14 shows the imaging by focal length change for a two-dimensional lens in the dynamic imaging experiment. The object is a resolution chart and the shown is the central part. Figure 14(a) represents the image of the resolution chart with a $2\text{mm} \times 2\text{mm}$ electro-optic lens being applied a voltage of 240 V. Figure 14(b) gives the situation when the voltage is taken off. Figure 14(c) shows the situation when a $3\text{mm} \times 3\text{mm}$ electro-optic lens with a 330 V applied voltage. Similar result was obtained when the image plane is fixed and the input object at an arbitrary plane can be imaged onto this plane by applying a proper voltage on the E-O lens. This demonstrates the situation for stored information retrieval. Situation is similar to that shown in Figure 13. The most right hand "image plane" will be the information to be retrieved, which may be anywhere within the "image range". A diffusing light was used to simulate the fluorescent light presence of a real two-photon absorption memory. Voltage is applied on the E-O lens in order to obtain a clear image on the "input object" plane. From here we see when a large aperture lens is used, the resolution of the dynamic image becomes better but high voltage is needed. There should be a compromise between a large aperture lens and a lower applied voltage in application. In the experiment, the focal point change is over 1 meter. In 3-D memory applications, the necessary change will not be greater than several centimeters, thus the needed applied voltage will be just several tens of volts. It is noted that because of the small relative aperture of the electro-optic lens in this experiment, some high frequency components of the input image are lost during the imaging. This will be improved when the system is optimized and compacted.

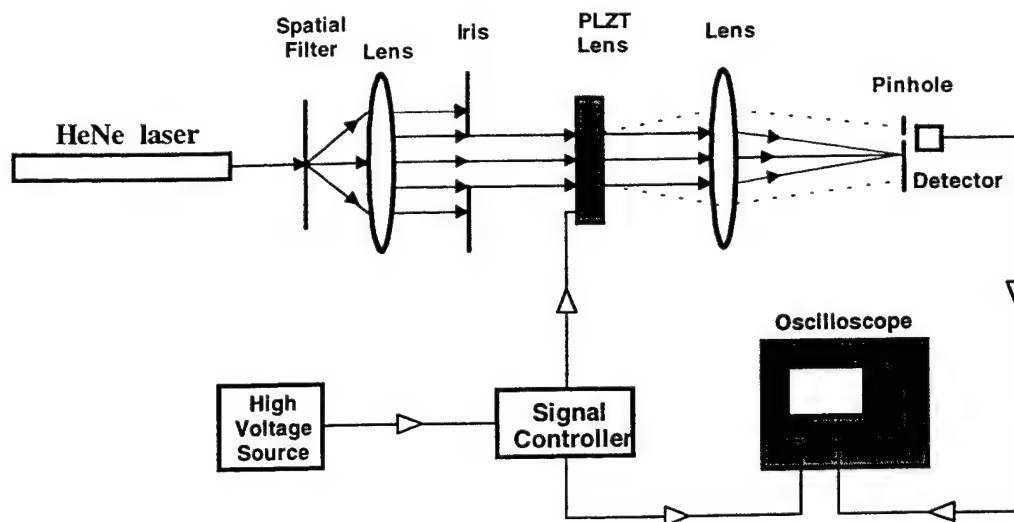


Figure 15. Setup utilized to measure the response time of the device.

The time response is an important performance parameter for an electro-optic device in application. To measure the time response of the device, we set up a system as shown in Figure 15. The experiment was performed on the 2mm×2mm wide device. The device was driven by a high voltage supply which was modulated by a step function. The photodetector has a good frequency response up to 3GHz. At 400V, the rise time of the applied voltage was measured to be within 1.5 μ s on a Hewlett Packard 54503H digital oscilloscope. We also monitored the temporary current flow through the device after the step voltage is put on. The time between the initialization and the vanish of the charging current is 20 μ s. Device time response of 10 μ s is measured by detecting the beam spot reaction time to the signal.

PLZT itself has an intrinsic time response less than 1 μ s, and the time response of the device depends mainly on the value of the resistance of the metal electrodes and the parasitic capacitance between the top surface and the back surface. The use of the metal electrodes has advantages over ITO transparent interdigital electrodes arrangement. In the later case, the sheet resistivity is hard to be lowed to produced a comparable result with the metal one. The resistance of the metal outlines can be further decreased by increasing the metal lines deposition thickness or using a more conductive metal like copper or gold, thus yielding a decrease in response time.

5.4) Mathematical description of the electro-optic process

Previous mathematical expression is not the real case but a well approximation. Actually there is also a transverse component of the electrical field, which though small will influence the result and result in aberrations. We iterate define the coordinate system here. Principal axes x and z lie in the top surface of the PLZT and are perpendicular and parallel to the electrodes, respectively. Axis y points into the PLZT wafer. The mathematical expression of the complete electro-optic effect inside the PLZT substrate is as follows. Boundary conditions for the voltage distribution inside the PLZT substrate are given by

$$V(x,0) = \begin{cases} 0, & |x| \leq \frac{a}{2}, \\ \frac{2|x| - a}{W - a} V, & \frac{a}{2} < |x| \leq \frac{W}{2}, \\ V, & \frac{W}{2} < |x| \leq \frac{W}{2} + d, \end{cases} \quad (5-8)$$

and

$$V(x,t) = 0. \quad (5-9)$$

We extend the boundary condition to a periodic one, so that the boundary condition at $y=0$ is given by

$$V(x + n(W + 2d), 0) = V(x, 0), \quad (5-10)$$

as shown in Figure 16, where n is an integer.

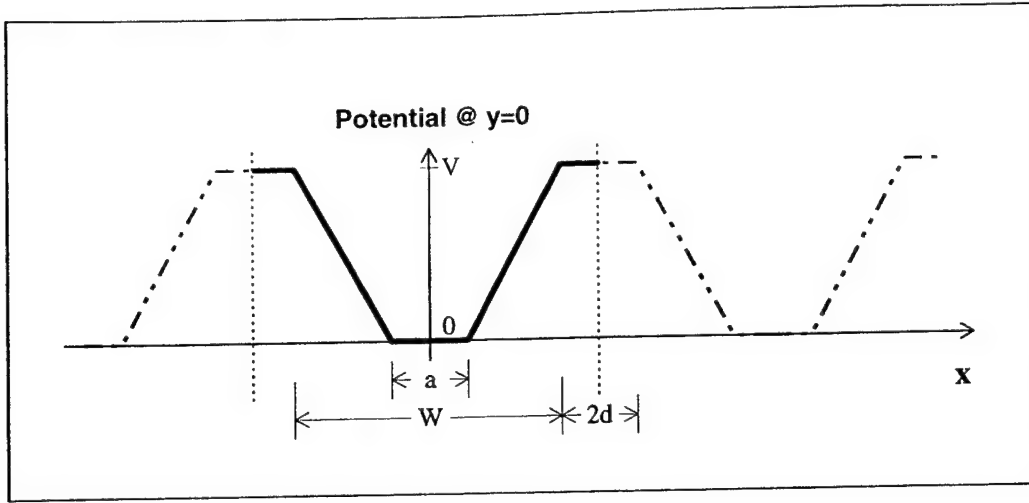


Figure 16. Potential boundary condition at the top surface of the PLZT substrate.

We can have the $y=0$ boundary condition been decomposed into Fourier series as expressed below

$$V(x,0) = V_0 + \sum_{n=1}^{\infty} P(\xi_n) \cos(\xi_n x), \quad (5-11)$$

where

$$\xi_n = \frac{2n\pi}{W+2d}, \quad (5-12)$$

$$V_0 = \frac{1}{W+2d} \int_{-(\frac{W}{2}+d)}^{\frac{W}{2}+d} V(x,0) dx, \quad (5-13)$$

$$P(\xi_n) = \frac{2}{W+2d} \int_{-(\frac{W}{2}+d)}^{\frac{W}{2}+d} V(x,0) \cos(\xi_n x) dx. \quad (5-14)$$

Combining the potential boundary conditions of Equations (5-9) and (5-11), we can assume a trial solution for the potential distribution inside PLZT

$$V(x,y) = \left(1 - \frac{y}{t}\right) V_0 + \sum_{n=1}^{\infty} P(\xi_n) \cos(\xi_n x) \frac{\sinh[\xi_n(t-y)]}{\sinh(\xi_n t)}. \quad (5-15)$$

The electrical field distributions can be obtained by taking the gradient of the above voltage distribution as given by

$$E_x(x,y) = -\frac{\partial V(x,y)}{\partial x} = \sum_{n=1}^{\infty} \xi_n P(\xi_n) \sin(\xi_n x) \frac{\sinh[\xi_n(t-y)]}{\sinh(\xi_n t)}, \quad (5-16)$$

$$E_y(x, y) = -\frac{\partial V(x, y)}{\partial y} = \frac{V_0}{t} + \sum_{n=1}^{\infty} \xi_n P(\xi_n) \cos(\xi_n x) \frac{\cosh[\xi_n(t-y)]}{\sinh(\xi_n t)}. \quad (5-17)$$

The refractive indices of the PLZT at an arbitrary location inside the wafer are expressed as

$$n_x(x, y) = n_0 - \frac{1}{2} n_0^3 [R_{11} E_x^2(x, y) + R_{12} E_y^2(x, y)], \quad (5-18)$$

$$n_y(x, y) = n_0 - \frac{1}{2} n_0^3 [R_{12} E_x^2(x, y) + R_{11} E_y^2(x, y)], \quad (5-19)$$

$$n_z(x, y) = n_0 - \frac{1}{2} n_0^3 R_{12} [E_x^2(x, y) + E_y^2(x, y)]. \quad (5-20)$$

The index of refraction for the z -polarized light, whose polarization is parallel to the electrodes, is $n_z(x, y)$. The refractive index for the x -polarized light, whose polarization is perpendicular to the electrodes, is $n_x(x, y)$. With the indices available, the phase modulation for the x - and z -polarized light can be written as

$$\phi_x(x) = \frac{2\pi}{\lambda} \int_0^t n_x(x, y) dy, \quad (5-21)$$

$$\phi_z(x) = \frac{2\pi}{\lambda} \int_0^t n_z(x, y) dy, \quad (5-22)$$

where λ is the laser wavelength.

5.5) Computer evaluation of device aberration

A computer simulation was generated. We use Equations (5-21) and (5-22) for the phase retardation evaluation. A perfect lens should have a quadratic phase factor, or there would be aberrations. Parameters used for the simulations are as follows: $R_{11} = 4.00 \times 10^{-16} \text{ m}^2/\text{V}^2$, $R_{12} = -2.42 \times 10^{-16} \text{ m}^2/\text{V}^2$, $W = 2.00 \text{ mm}$, $a = 4.0 \text{ } \mu\text{m}$, $d = 100.0 \text{ } \mu\text{m}$, and $t = 0.32 \text{ mm}$.

We followed the complete physical principles for the electro-optic effect of the quadratic PLZT ceramic in the simulation and determined the field distribution inside the PLZT by applying boundary conditions as shown in Equations (5-8) and (5-9). To ease the mathematical derivation, we use the digital fast Fourier transform (FFT) on the

voltage distribution expressed by Equations (5-8) and (5-10). This assumption assures that the potential along the $x=0$ line and $x=W/2+d$ line are always the minimum and maximum at any x - z plane.

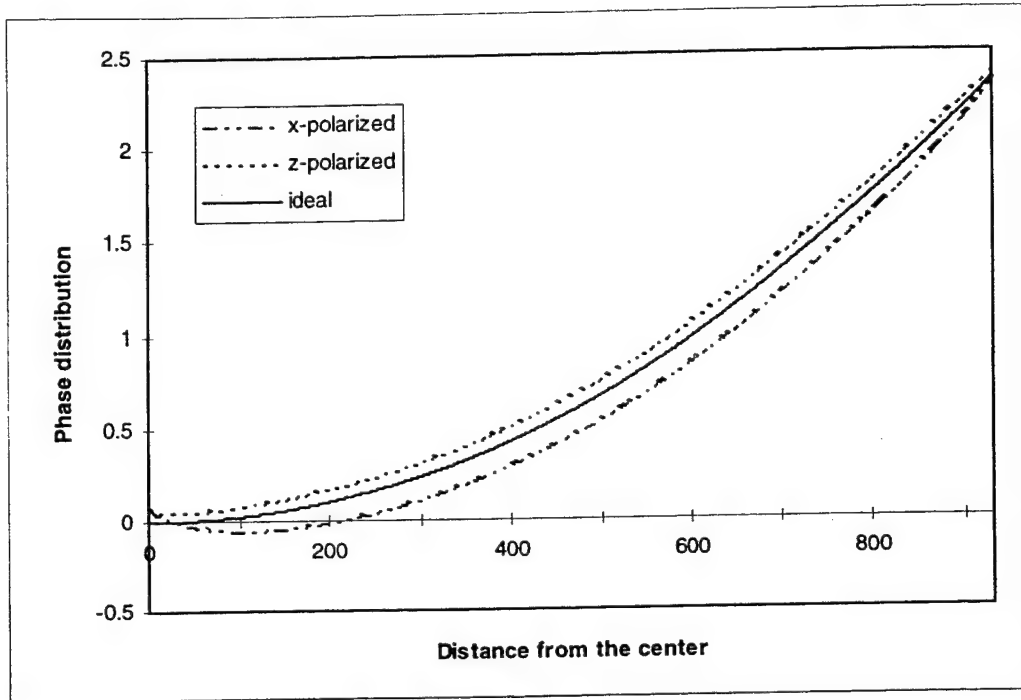
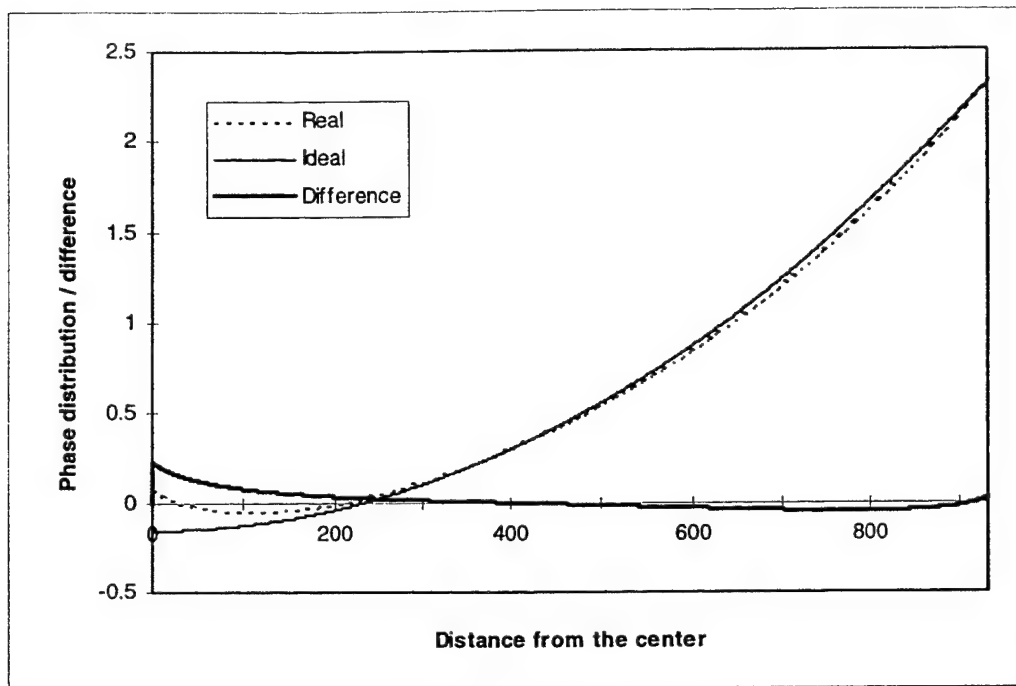


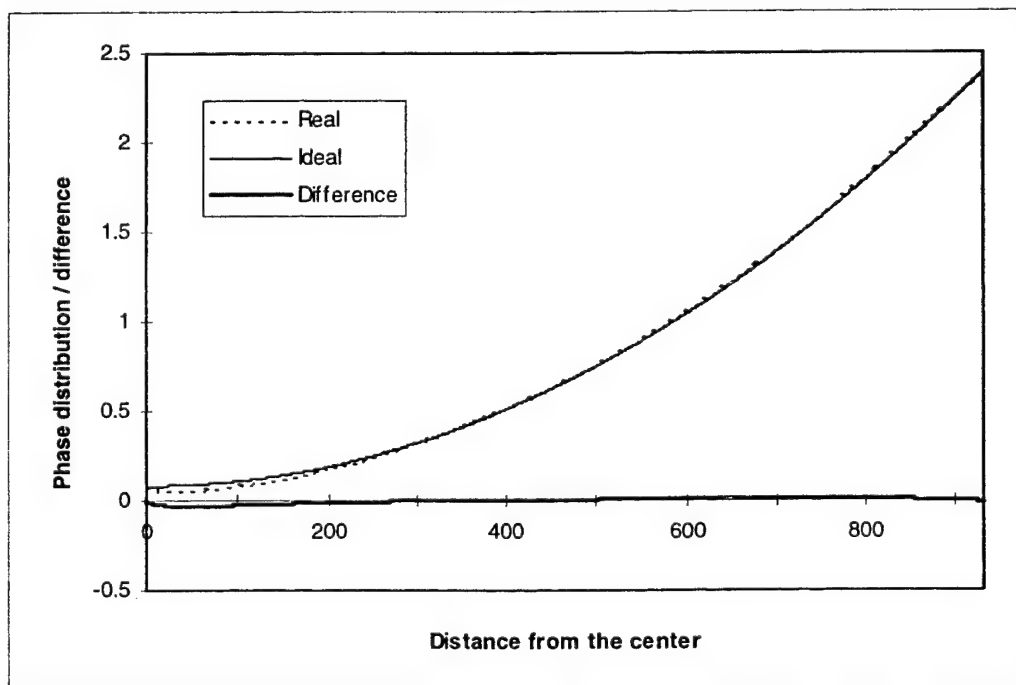
Figure 17. Comparison of x- and z-polarized phase distributions with that of the ideal case at 200 V.

The simulated actual and ideal cases are shown in Figure 17. The horizontal axis of the diagram represents the x axis of the device, while vertical represents the corresponding phase retardation. The range in x in this figure represents 1mm. Because of the unwanted transversal field components, the phase retardation for the z -polarized light is greater than the ideal case while the case for x -polarized light is lower than the ideal one. The difference among these three cases can be reduced by using a thinner PLZT wafer or by using a larger lens aperture. That is, when we use large apertures, the difference can be really ignored. Actually a quadratic curve with a constant bias also represents an ideal lens. Figure 18 compares the real cases for x - and z -polarized light and

a closest biased ideal case. For the z-polarized light, this device behaves much similar to an ideal lens, as shown in Figure 18 (b).



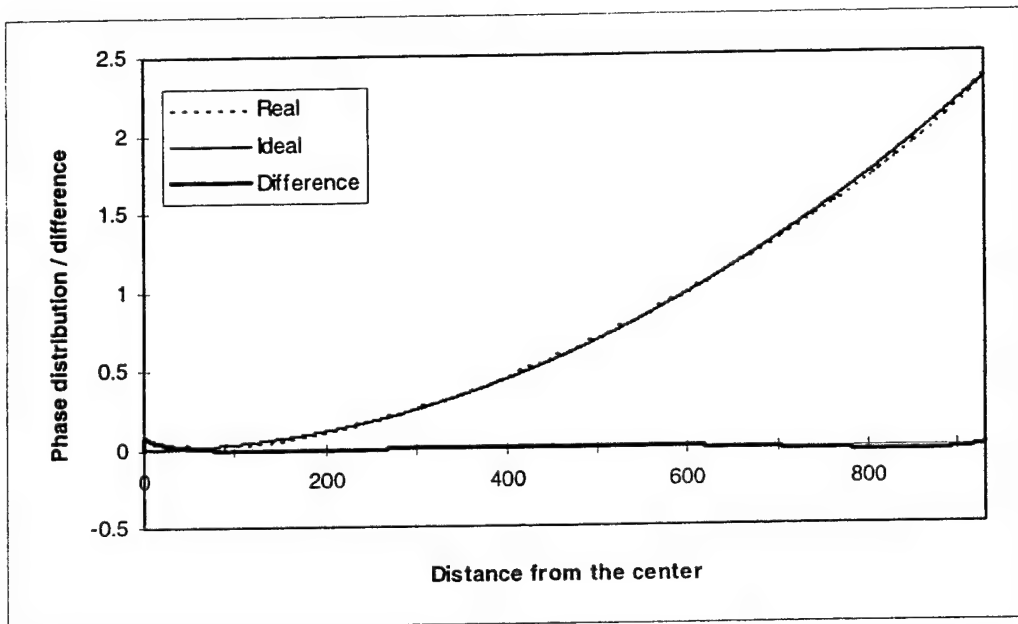
(a)



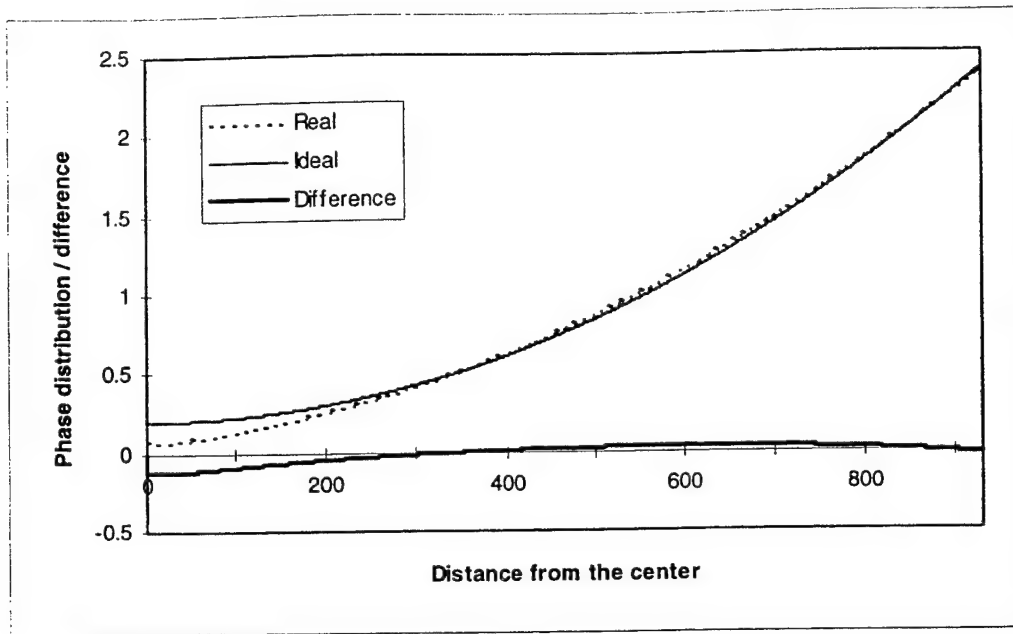
(b)

Figure 18. Comparison of a) x-polarized and b) z-polarized light phase distribution with that of an ideal case at 200 V.

A similar case is found for x-polarized light when the center electrode is given a certain bias voltage. Figure 19 gives a similar case as Figure 18 except that a portion of the applied voltage was dropped between the central electrode and the ground. Figure 19(a) shows that x-polarized light experiences an almost ideal lens. Aberration exists only near the center electrode, where 0.1 bias means that 1 out of 10 in the applied voltage is used as the bias on the electrical electrode and the ground while the other 9 of 10 applied on the outer and central electrodes.



(a)



(b)

Figure 19. Comparison of a) x-polarized and b) z-polarized light phase distribution with that of an ideal case at 200 V and a bias of 0.1 on the center.

It should be pointed out that aberrations for x - and z -polarized light can not be corrected simultaneously because the nature of the polarization. For the two quadratic coefficients are sign opposite, when we correct one aberration, the other will become larger than before. This suggests that the lens is polarization sensitive. But in most of the cases, laser is used as the illumination which is usually linearly polarized.

6. Scaleless dynamic imaging system: optical memory recording and retrieval

The line-of-light concept demonstrates a scanning line controlled by electrical signals. Actually it also demonstrates of a one-dimensional dynamic imaging provided that a one-dimensional spatial light modulator (SLM) is placed at the back focus plane of the cylindrical lens. This one-dimensional imaging is required for the line-by-light oriented information recording. On the other hand, a two-dimensional dynamic recording system is also desired in such three-dimensional optical memory system as holographic recording etc.

Figure 20 shows a system of demonstrating our idea of line of light 3-D optical memory. Beam 1 is the information bearing arm of the recording system. A matrix SLM is used to display the input image. The two Fourier lenses form a 4-f system with a two-dimensional PLZT electro-optic lens at the Fourier plane. The input page information is imaged (following the arrows from left to right) by the three devices onto a plane inside the recording medium at the right-hand side of the figure. When a voltage is applied to the PLZT lens, the imaging plane moves back and forth along the optical axis of the system thus permitting dynamic three-dimensional recording. The applied voltage can be generated from a computer-controlled address controller which determines which input page to choose and where it is imaged. When the imaging plane moves, the image size keeps unchanged.

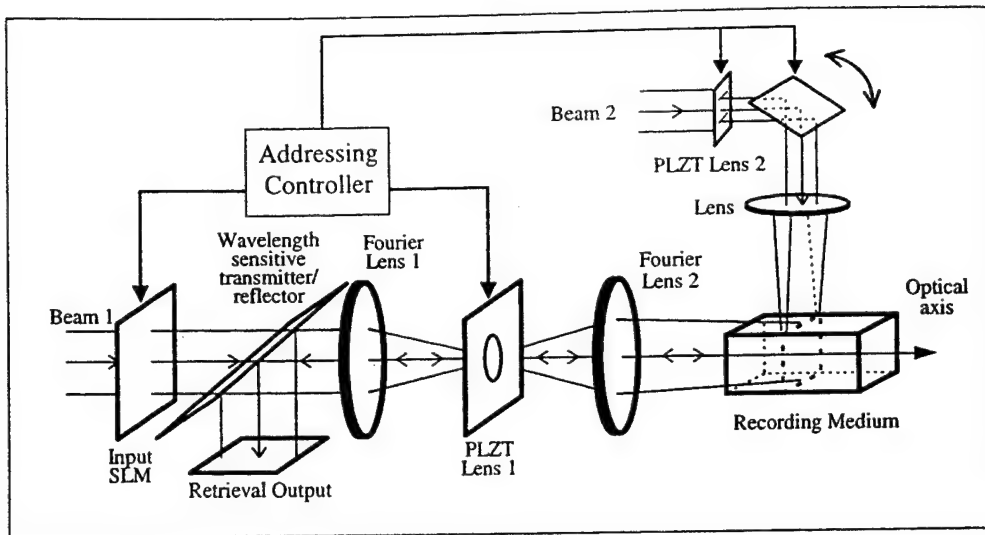


Figure 20. Proposed system for 3-D memories information storage and retrieval. Stress is on the beam 1 configuration.

Beam 2 is used as the reference beam to produce a scanning line-of-light. The basic structure of this part is similar to that in Figure 4 except the rotating mirror. The use of the PLZT electro-optic lens enables the line-of-light to move along the optical axis. The mirror is used to move the line perpendicular to the optical axis. Thus the whole block of the recording medium could be covered. The rotating mirror can be replaced by an acousto-optic reflector controlled by electrical signals. When the recording is performed, a line information is displayed on the input SLM. The PLZT lens 1 adjust its focal length to image that line information onto a certain place in the recording medium. PLZT lens 2 and the acousto-optic modulator act accordingly to produce a line of light to coincide with the image of the line information. Therefore a line of information is recorded.

This system can also be used for the information retrieval purpose. Beam 1 is blocked; PLZT lens 2 and the acousto-optic lens conduct beam 2 to retrieve a line of information. The emitted fluorescent light from the recording medium travels back to the left (following the arrows from right to left). A corresponding voltage is applied onto the PLZT lens 1. Thus the retrieved data is displayed at the retrieval output plane through the wavelength sensitive reflector. The wavelength sensitive transmitter/reflector is transparent to the wavelength of Beam 1 in the recording session and reflects the

fluorescent light emitted from the recording media in the retrieval session since the emitting light of the recording media is different from the recording laser beam. Fast electrical operation ability also makes the system programmable and easy to operate. The non-mechanical structure avoids movement of any element in the system so that there will be no worn-out and thus the possibility of an error to occur will be greatly reduced. Both the forward and backward dynamic imaging have been realized and demonstrated to the inspecting sponsor.

A conservative estimation gives that our current technique can achieve a storage capacity of 1.0 G bit for a $1.0 \times 1.0 \times 1.0 \text{ cm}^3$ cubic material providing that the recording unit is $10 \times 10 \times 10 \text{ }\mu\text{m}^3$. The retrieval throughput is determined by the time response of the PLZT lens, which was measured at $10 \text{ }\mu\text{s}$. Thus reading the whole block needs $10 \times 10^6 \text{ }\mu\text{s}$. That is a speed of 100M bit/s. As we have claimed, this is a conservative estimation. The improvement is achievable with further research and revisions of the PLZT lens or the availability of new materials.

7. Discussions and conclusions

In conclusion, we have presented the fulfillment of the contract. We proposed the line-of-light concept to replace the sheet-of-light using the PLZT electro-optic variable lenses produced in this project. The design of the lens takes advantage of the intrinsic quadratic electro-optic effect of the material. The design takes a simple form and is almost free of diffraction loss. A converging zoom lens can be achieved by combining this device with a conventional lens. A layer of amorphous germanium as thin as what we used is quite transparent but an amorphous silicon layer may produce better result. Reference¹¹ claimed that n+ amorphous silicon can produce a sheet resistivity of 16 M Ω /sq. at the thickness of 1 μ m, which is in the range of our need. Using this material is expected to have an easier control of the sheet resistance. Therefore, it is possible to control the thickness of the resistive layer so that it also functions as a quarter wavelength antireflection coating. Dynamic imaging experiment shows that with the help of a conventional convex lens and a voltage up to 300 V, the image plane of the combined imaging system can be moved back and forth up to several tens of centimeters. This is more than enough for most 3-D memory applications.

The investigation has demonstrated on a limited basis that solid state electro-optic lenses can be applied to 3-D memories to fully stress fast parallel data accessibility of the optical system. Random access of data is implemented by applying to the device a control voltage with a value corresponding to the data position. This access can be completed in several micro-seconds or less. The implementation of a dynamic imaging system will enable the automation of the 3-D memories through a host programmable controller, which gives commands for system operation and program the data storage and retrieval processes.

8. References

- [1] S. Esener, J. E. Ford and S. Hunter, "Optical data storage and retrieval: research directions for the 90's," *Optical Technologies for Aerospace Sensing - Critical Reviews of Optical Science and Technology*, J. E. Person, Ed., SPIE Volume **CR47**, 94-130 (1993).
- [2] A. S. Dvornikov and P. M. Rentzepis, "2-photon 3-dimensional optical storage memory," *Advances in Chem.* **240**, 161-177 (1994).
- [3] G. H. Haertling, "PLZT electro-optic materials and applications - a review," *Ferroelectrics*, **75**, 25-55 (1987).
- [4] H. Sato, T. Tatebayashi, T. Yamamoto, and K. Hayashi, "Electro-optic lens composed of transparent electrodes on PLZT ceramic towards optoelectronic devices," In *Optics in Complex Systems*, F. Lanzl, H. Preuss, and G. Weigolt, eds., *Proc. Soc. Photo-Opt. Instrum. Eng.* **1319**, 493-494 (1990).
- [5] T. Tatebayashi, T. Yamamoto, and H. Sato, "Electro-optic variable focal-length lens using PLZT ceramic," *Appl. Opt.* **30**, 5049-5055 (1991).
- [6] Tsuyoshi Tatebayashi, Takashi Yamamoto, and Heihachi Sato, "Dual focal point electrode-optic lens with a Fresnel-zone plate on a PLZT ceramic," *Appl. Opt.* **31**, 2770-2775 (1992).
- [7] Q. Wang Song, X.-M. Wang and R. Bussjager, "Lanthanum-modified lead zirconate titanate ceramic wafer-based electro-optic dynamic diverging lens," *Opt. Lett.* **21**, 242-244 (1996).
- [8] Q. Wang Song, Xu-Ming Wang, and Fred Haritatos, "Test and analysis of an electro-optic dynamic diverging lens for three-dimensional optical memories," *Appl. Opt.* **36**, 1796-1803 (1997).
- [9] G. H. Haertling, "PLZT electrooptic ceramics and devices," in *Industrial Applications of Rare Earth Elements*, K. A. Gschneidner, Jr. Ed., ACS Symposium Series, **164**, 265-283 (1981).

- [10] D. H. Goldstein, "PLZT modulator characterization," *Opt. Eng.* **34**, 1589-1592 (1995).
- [11] N. A. Riza and M. C. DeJule, "Three-terminal adaptive nematic liquid-crystal lens device," *Opt. Lett.* **19**, 1013-1015 (1994).

MISSION OF ROME LABORATORY

Mission. The mission of Rome Laboratory is to advance the science and technologies of command, control, communications and intelligence and to transition them into systems to meet customer needs. To achieve this, Rome Lab:

- a. Conducts vigorous research, development and test programs in all applicable technologies;
- b. Transitions technology to current and future systems to improve operational capability, readiness, and supportability;
- c. Provides a full range of technical support to Air Force Material Command product centers and other Air Force organizations;
- d. Promotes transfer of technology to the private sector;
- e. Maintains leading edge technological expertise in the areas of surveillance, communications, command and control, intelligence, reliability science, electro-magnetic technology, photonics, signal processing, and computational science.

The thrust areas of technical competence include: Surveillance, Communications, Command and Control, Intelligence, Signal Processing, Computer Science and Technology, Electromagnetic Technology, Photonics and Reliability Sciences.